Supporting information

A simple fabrication of multifunctional inorganic paper with high efficiency separations for both liquids and particles

Gang Wen,[a,b#] Xiaoyu Gao,[a,b#] ZhiGuang Guo[a,b*]

[a.] *Hubei Collaborative Innovation Centre for Advanced Organic Chemical Materials and Ministry of Education Key Laboratory for the Green Preparation and Application of Functional Materials, Hubei University, Wuhan 430062, People's Republic of China*

[b.] *State Key Laboratory of Solid Lubrication, Lanzhou Institute of Chemical Physics, Chinese Academy of Sciences, Lanzhou 730000, People's Republic of China.*

[#] *These authors contributed equally to this work*

E-mail: zguo@licp.cas.cn; Fax: +86-931-8277088; Tel.: +86-931-4968105

Flexible test of HAP@NH_2-UiO-66. (Movie S1)

Dynamic meausrements of water spreading of raw paper. (Movie S2)

Dynamic meausrements of water spreading of HAP@NH_2-UiO-66. (Movie S3)

Dynamic meausrements of underwater oil-adhesion on the surface of HAP@NH_2-UiO-66. (Movie S4)

Surfactant-stabilized petroleum ether-in-water emulsion separation. (Movie S5)

Surfactant-stabilized n-octane-in-water emulsion separation. (Movie S6)

Surfactant-stabilized dichloroethane-in-water emulsion separation. (Movie S7)

PMs dynamic filtration test of HAP@NH_2-UiO-66. (Movie S8)

Fire-resistant property of HAP@NH_2-UiO-66. (Movie S9)

MB adsorption experiment on HAP@NH_2-UiO-66. (Movie S10)

MO adsorption experiment on HAP@NH_2-UiO-66. (Movie S11)

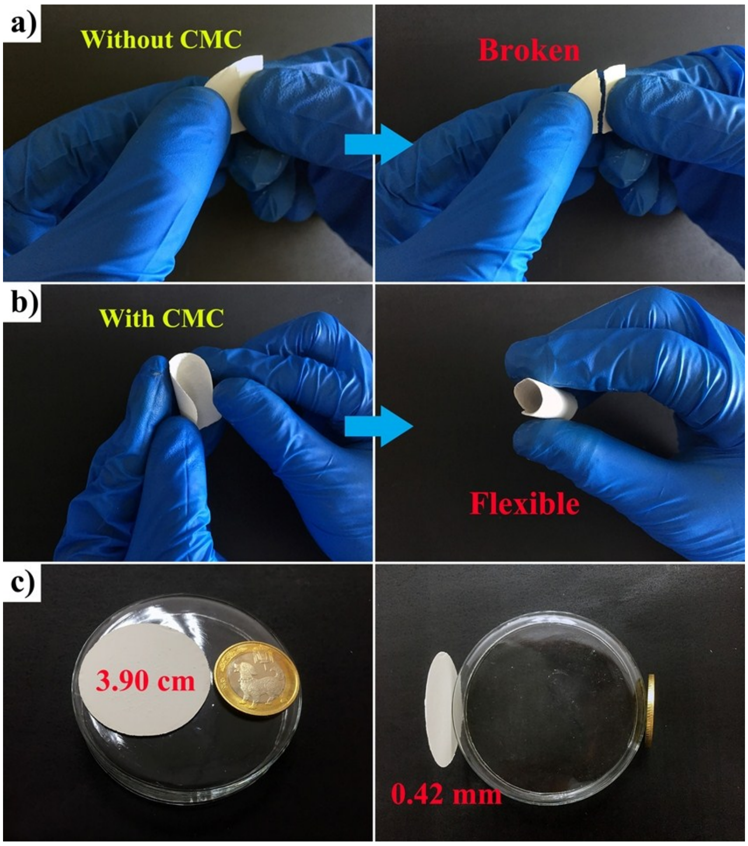

Fig. S1 Photographs showing a) paper without CMC and b) paper with CMC. The paper without CMC becomes scattered and is easy to be broken. The paper with CMC is flexible and can be rolled up easily.

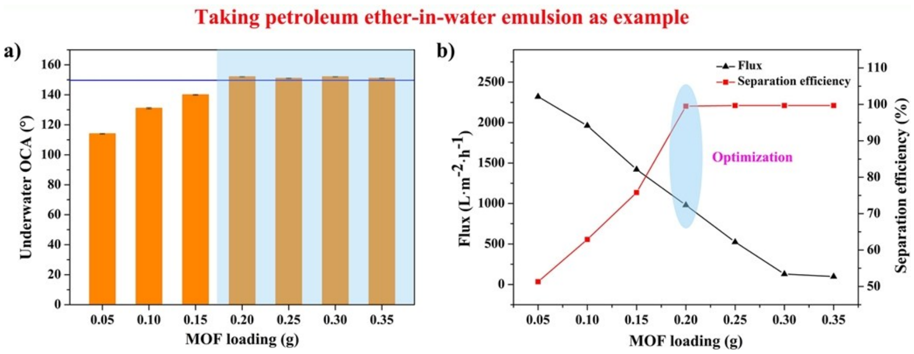

Fig. S2 Taking petroleum ether-in-water emulsion as example. a) The relationship of underwater OCA and different loading of NH_2-UiO-66 on HAP. b) The influence of flux and separation efficiency toward different NH_2-UiO-66 loading on HAP.

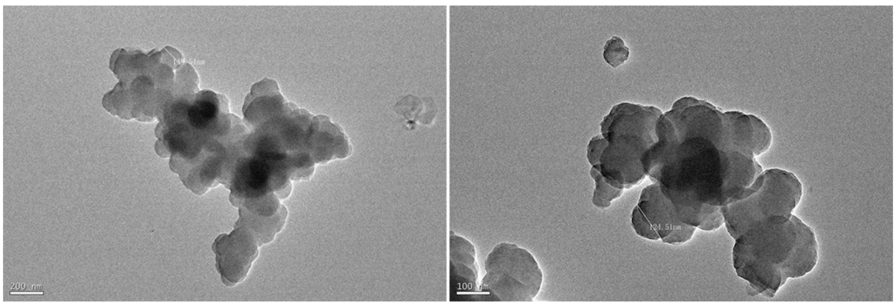

Fig. S3 TEM images of NH_2-UiO-66.

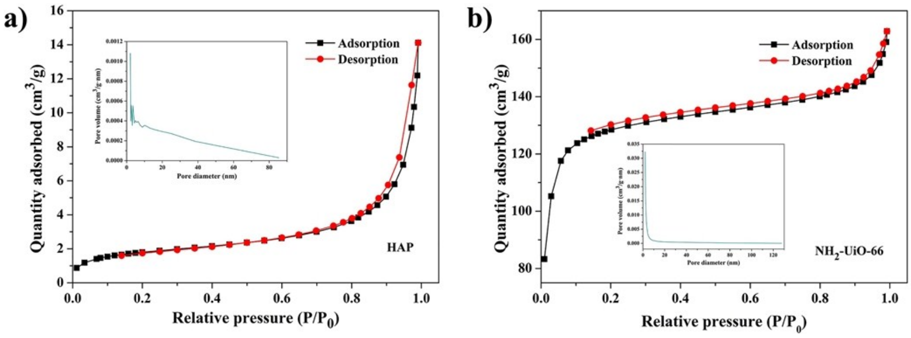

Fig. S4 N_2 adsorption/desorption isotherms and sizes distribution curves (inset) of a) HAP and b) HAP@NH_2-UiO-66.

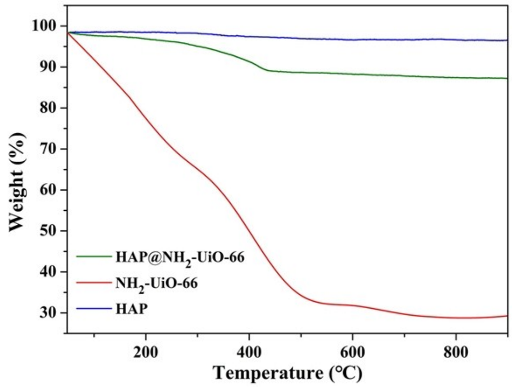

Fig. S5 TG curves of HAP, NH_2-UiO-66 and HAP@NH_2-UiO-66.

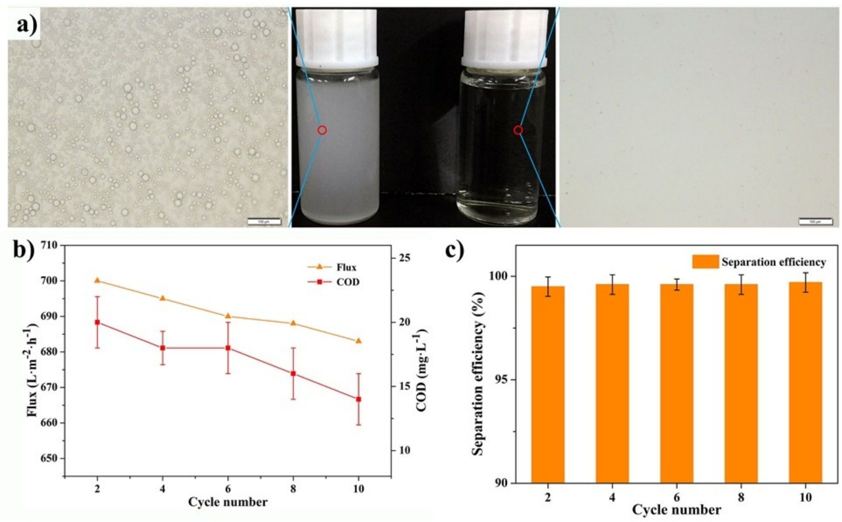

Fig. S6 a) Optical microscopy images of surfactant-stabilized n-Octane-in-water emulsion (left) and the collected filtrate (right). b) Flux of surfactant-stabilized n-Octane-in-water emulsion separation and COD values in the collected filtrates. c) Separation efficiency of surfactant-stabilized n-Octane-in-water emulsion. One experiment consists of 2 complete cycles.

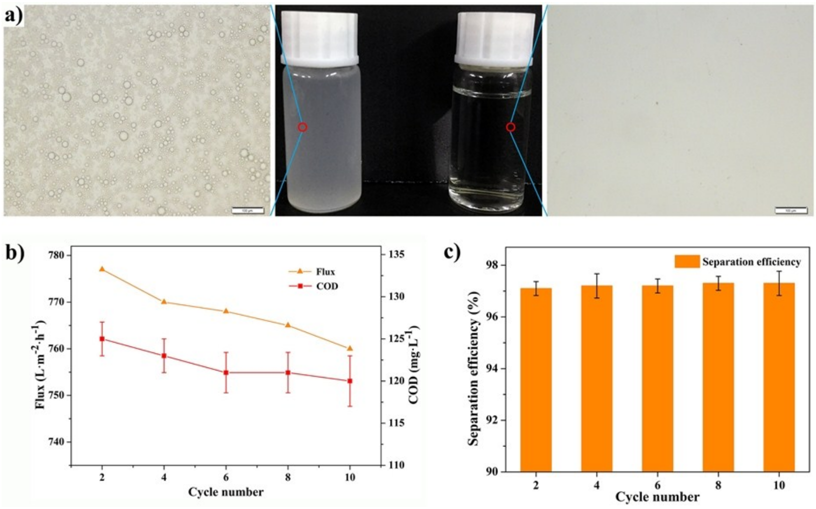

Fig. S7 a) Optical microscopy images of surfactant-stabilized Dichloroethane-in-water emulsion (left) and the collected filtrate (right). b) Flux of surfactant-stabilized Dichloroethane-in-water emulsion separation and COD values in the collected filtrates. c) Separation efficiency of surfactant-stabilized Dichloroethane-in-water emulsion. One experiment consists of 2 complete cycles.

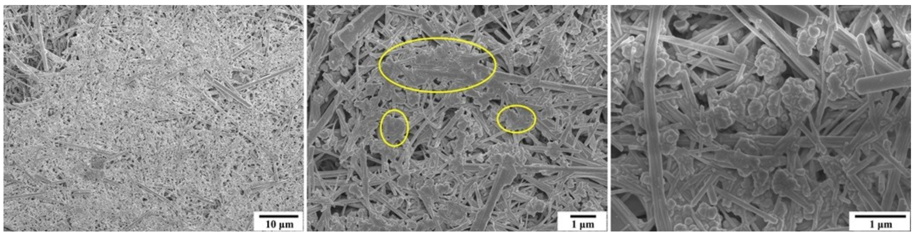

Fig. S8 SEM images of HAP@NH_2-UiO-66 after PMs removal (windward surface).

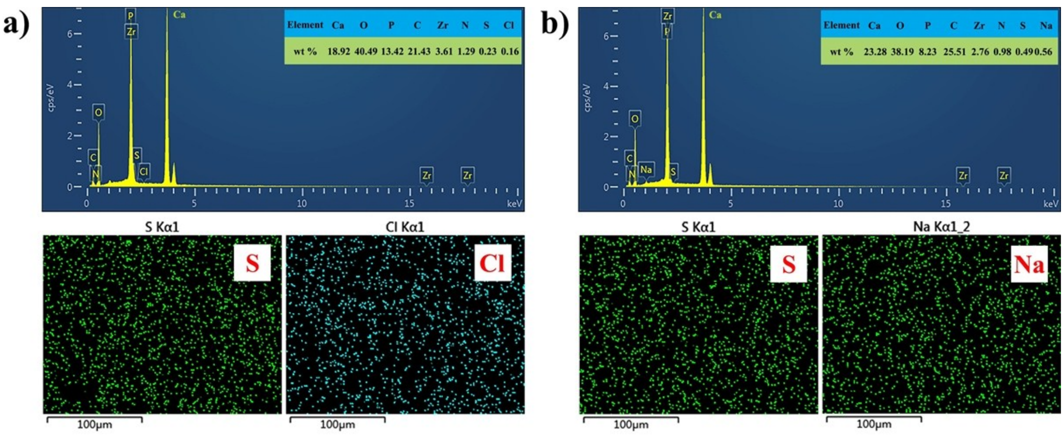

Fig. S9 a) EDS spectra and FESEM-EDS mapping of HAP@NH_2-UiO-66 after MB dye adsorption. b) EDS spectra and FESEM-EDS mapping of HAP@NH_2-UiO-66 after MO dye adsorption.

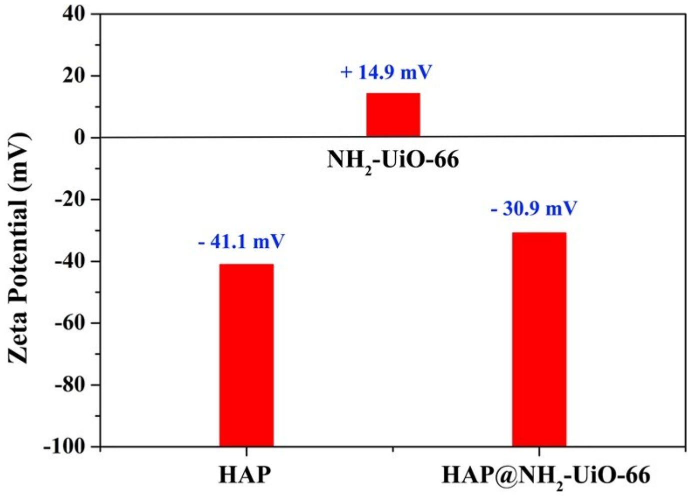

Fig. S10 Zeta potential of HAP, NH_2-UiO-66 and HAP@NH_2-UiO-66.

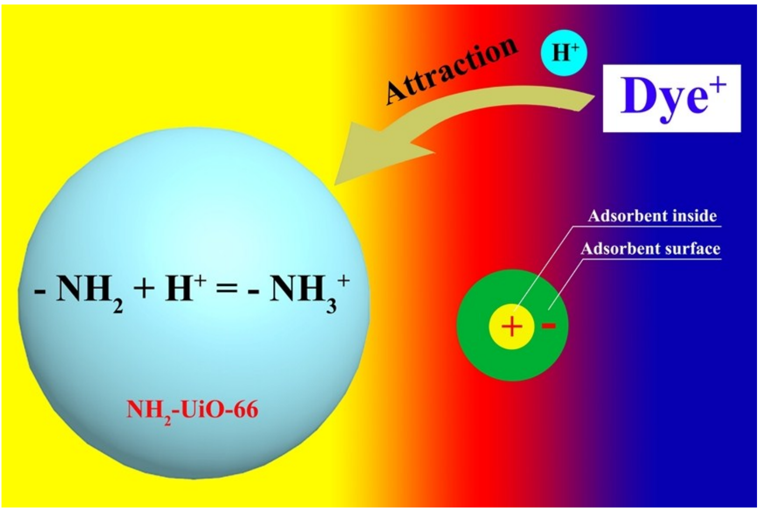

Fig. S11 Mechanism diagram of MB adsorption on the surface of HAP@NH_2-UiO-66.